Gator: a Python-driven program for spectroscopy simulations using correlated wave functions

Dirk R. Rehn,[*] Zilvinas Rinkevicius,[†‡] Michael F. Herbst,[§] Xin Li,[†] Maximilian Scheurer,[*] Manuel Brand,[†] Adrian L. Dempwolff[*] Iulia E. Brumboiu,[†,¶] Thomas Fransson,[*,‖] Andreas Dreuw,[*] Patrick Norman[†]

Article Type:

Software Focus

Abstract

The Gator program has been developed for computational spectroscopy and calculations of molecular properties using real and complex propagators at the correlated level of wave function theory. At present, the focus lies on methods based on the algebraic diagrammatic construction (ADC) scheme up to third-order of perturbation theory. A Fock matrix-driven implementation of the second-order ADC method for excitation energies has been realized with an underlying hybrid MPI/OpenMP parallelization scheme suitable for execution in high-performance computing cluster environments. With a modular and object-oriented program structure written in a Python/C++ layered fashion, Gator enables, in addition, time-efficient prototyping of novel scientific approaches as well as interactive notebook-driven training of students in quantum chemistry.

[*]Interdisciplinary Center for Scientific Computing, Ruprecht-Karls University, Im Neuenheimer Feld 205, 69120 Heidelberg, Germany

[†]Department of Theoretical Chemistry and Biology, School of Engineering Sciences in Chemistry, Biotechnology and Health, KTH Royal Institute of Technology, SE-106 91 Stockholm, Sweden

[‡]Department of Physics, Faculty of Mathematics and Natural Sciences, Kaunas University of Technology, Kaunas LT-51368, Lithuania.

[§]CERMICS, École des Ponts ParisTech, 6 & 8 avenue Blaise Pascal, 77455 Marne-la-Vallée, France; Inria Paris, 75589 Paris Cedex 12, France

[¶]Department of Chemistry, Korea Advanced Institute for Science and Technology, 34141 Daejeon, Korea

[‖]Fysikum, Stockholm University, Albanova, SE-106 91 Stockholm, Sweden

GRAPHICAL TABLE OF CONTENTS

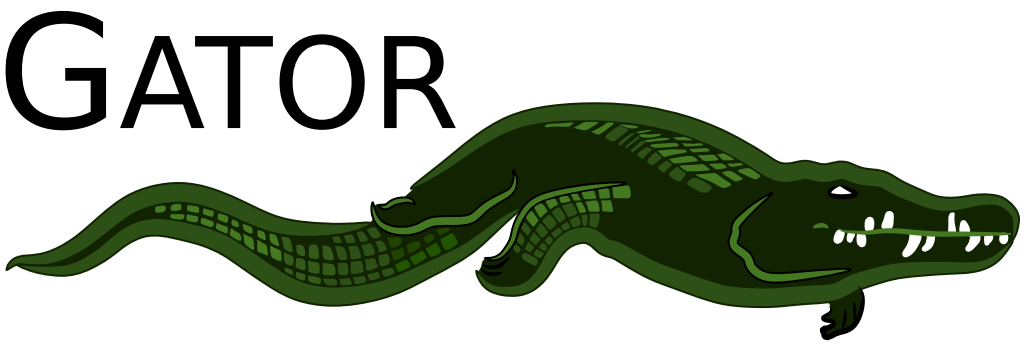

Caption: The Gator program is an easy-to-use yet powerful tool to calculate molecular properties and spectroscopies with real and complex response functions using the second- and third-order algebraic diagrammatic construction scheme.

INTRODUCTION

Quantum chemical calculations have become a corner stone for fundamental and applied research in molecular sciences. Simulations of spectroscopies and predictions of molecular properties are made available through various formulations of response theory and allow for the revelation of molecular structure–function relationships that are indispensable for experimental spectrum characterization and rational material design (Norman, Ruud, & Saue, 2018; Grunenberg, 2010). However, any attempt to compute molecular spectra and/or properties remains a compromise between accuracy and applicability—in particular so for large molecular systems embedded in complex environments (P. H. P. Harbach & Dreuw, 2011)—and while reliable quantum chemical methods exist to address the electronic ground state, electronic structure theory as a whole and efficient computer programs in particular are lagging behind the current needs in the field of computational spectroscopy (Gonzalez, Escudero, & Serrano-Andres, 2011). A wide range of semi-empirical and density-functional based methods exist and which are applicable to a wide range of large molecular systems (Holthausen & Koch, 2001; Mardirossiana & Head-Gordon, 2017), but they are not reliable and predictive without extensive benchmarking and/or comparison to experiment. This turns out to be an increasingly difficult way forward with growing system complexity as

suitable experiments are often missing and highly accurate methods are computationally unaffordable (Dreuw, 2006). Therefore, the development of wave function-based *ab initio* methods and the provision of efficient computer program implementations are in high demand, not least since such methods are systematically improvable and usually demonstrate a predictive power. In contrast to semi-empirical and density-functional based approximations, the physical effects contained in the *ab initio* Hamiltonian are *a priori* well defined and it is clear from the start, which properties and spectra can thus be described physically correct.

The focus of the Gator program lies on single-reference methods, currently using the algebraic diagrammatic construction (ADC) scheme for the polarization propagator, but further extensions are planned. In this first release version of the program, ADC is available up to third order in the fluctuation potential (Schirmer, 1982; Trofimov & Schirmer, 1995; P. H. Harbach, Wormit, & Dreuw, 2014; Dreuw & Wormit, 2015), as included in the ADC connect (adcc) module (Herbst, Scheurer, Fransson, Rehn, & Dreuw, 2020). Based on the capabilities of the adcc module, the Gator program implements linear real and complex response functions for the calculation of molecular properties. Moreover, the Gator project has the target ambition to enable *ab initio* quantum molecular modeling in high-performance computing (HPC) environments. In this first release version of the program, Møller–Plesset (MP) perturbation theory as well as ADC up to second order have been implemented with efficient exploitation of standard HPC cluster resources that are typically built from nodes with relatively small amounts of memory. This is accomplished using a distributed Fock matrix-driven ADC(2) tensor contraction scheme in a hybrid MPI/OpenMP parallel setting.

Overall, the Gator program is designed to provide a flexible platform for (i) high-performance *ab initio* quantum chemistry (ii) scientific extensions (methods and algorithms) with relative ease and quick turnover time and (iii) educational training with a high degree of student interactivity. These important program features are enabled with upper-level modules written in object-oriented Python that can be accessed in a notebook fashion. At the lower level, the program engine, represented by the hybrid massively parallel modules written in C++ for integral evaluation and transformation, allows for fast adaptation to contemporary and future general-purpose HPC resources.

With partly different scientific objectives but otherwise largely shared philosophy and intentions, similar program development efforts have recently been undertaken and served as inspiration for the present work: (i) the Massively Parallel Quantum Chemistry (MPQC) program package (Lewis, Calvin, & Valeev, 2016; Peng, Calvin, Pavosevic, Zhang, & Valeev, 2016; Peng et al., 2020) for *ab initio* simulations of the electronic structure of molecules and periodic solids; (ii) the PySCF program platform (Sun et al., 2018, 2020) for Python-based self-consistent field (SCF) and post-Hartree–Fock (post-HF) electronic structure theory calculations of finite and periodic systems; (iii) the Psi4NumPy (Smith et al., 2018, 2020) Python programming environment for facilitating use of the SCF and post-HF kernels from the Psi4 program through the NumPy library (van der Walt, Chris Colbert, & Varoquaux, 2011); (iv) the NWChem (Aprà et al., 2020) computational chemistry package designed and developed to work efficiently on massively parallel processing supercomputers; (v) the molsturm (Herbst, Dreuw, & Avery, 2018; Herbst, 2018) quantum-chemistry framework, which provides a contraction-based and basis-function independent SCF, integrating readily with existing integral libraries and post-HF codes; and (vi) the Dalton Project (J. M. H. Olsen et al., 2020) providing a platform written in Python for the interoperability of quantum chemical software projects.

PROGRAM STRUCTURE AND MODULARITY

Algorithmic considerations

The performance determining tasks in post-HF spectroscopy calculations are the atomic-to-molecular orbital integral transformation followed by the tensor operations defined in the iterative solution of the underlying response equations. Conventional implementations suited for shared-memory computers typically store the full tensor of transformed anti-symmetrized two-electron integrals in memory. While this approach works well also on standard computers for calculations on small systems, it quickly becomes unfeasible for medium- and large-scale systems due to the memory bottleneck. As a complement to a conventional integral transformation, we therefore also implement an MPI/OpenMP parallel Fock matrix-driven trans-

formation routine. The basic idea of this distributed integral transformation is to express quantities in the molecular orbital (MO) basis (such as integrals and tensor contractions) in terms of auxiliary Fock matrices.

For electron-repulsion integrals in the MO basis, we use the simple relation

$$\langle ij||kl\rangle = \sum_{\gamma,\delta}^{N} C_{\gamma k} F^{ij}_{\gamma\delta} C_{\delta l} - C_{\gamma l} F^{ij}_{\gamma\delta} C_{\delta k}, \tag{1}$$

where

$$F^{ij}_{\gamma\delta} = \sum_{\alpha,\beta}^{N} D^{ij}_{\alpha\beta} (\alpha\gamma|\delta\beta); \quad D^{ij}_{\alpha\beta} = C_{\alpha i} C_{\beta j}. \tag{2}$$

Here i, j, k, l and $\alpha, \beta, \gamma, \delta$ refer to MO and atomic orbital (AO) indices, respectively, and N is the number of basis functions. Using a split MPI communicator, the work of constructing the set of auxiliary Fock matrices is divided onto the available cluster nodes and any MO integral resulting from Eq. (1) remains on the node of its evaluation, ready *e.g.* for the distributed calculation of the MP2 energy.

For the ADC part, Gator relies on contraction-based iterative algorithms for solving response and eigenvalue equations. In such schemes, the ADC matrix $\mathbf{M}$ is never explicitly constructed but instead the secular and response equations are solved by calculating matrix–vector products with sets of trial vectors $\{b_i\}$:

$$\sigma_i = \mathbf{M} b_i. \tag{3}$$

In conventional implementations of the ADC(2) approach, these vectors consist of a single-excitation part and a much larger double-excitation part, which, however, can be folded into the space of single excitations (Hättig & Köhn, 2002), a technique known as partial renormalization. With contemporary standard cluster networks, vectors in the space of single excitations can be communicated between nodes with negligible effort and, within this space, expressions for the ADC(2) matrix–vector product in Eq. (3) have been derived and implemented in terms of auxiliary Fock matrices—an approach identical in idea but more complex in its details to the distributed calculation of the MP2 energy discussed above (the detailed expressions will be presented elsewhere).

For smaller systems the computational cost of the Fock-matrix driven approach is not beneficial and both variants of integral transformation and calculations of σ-vectors are

made available in the Gator program via a seamless integration with the VeloxChem program (Rinkevicius et al., 2020). In going beyond ADC(2), the Fock matrix-driven approach is presently not available. With an AO-integral screening based on a combination of the Cauchy–Schwarz inequality and the density, the calculation of Fock matrices scales somewhat better than N^3. As there are in total N^2 pair-indices (i, j), this results in a total scaling of less than N^5 for the Fock matrix-driven integral transformation in Eq. (1).

Modular structure of Gator

The Gator program consists of three major modules as illustrated in Figure 1: (i) *HPC-QC* for MP2 and ADC(2) calculations in HPC environments, exploiting the Fock-matrix driven integral transformation outlined above; (ii) *Respondo* for the evaluation of real and complex linear response functions and (iii) *ADC connect* (adcc) (Herbst et al., 2020) for excited state calculations based on the ADC scheme up to third order. The Hartree–Fock reference state and the required one- and two-electron integrals are provided by the VeloxChem (Rinkevicius et al., 2020) program but, owing to the modular and object-oriented software design, Gator can easily be interfaced also to other self-consistent field (SCF) programs.

In terms of program languages, the modules of Gator are developed in a two-layered fashion. The upper layer is written in Python 3 and contains the management of the hardware resources, input/output handling, and result processing as well as high-level parts of some algorithms. Here, numerical array operations are carried out either the NumPy or SciPy (Jones, Oliphant, & Peterson, 2001) libraries. The lower layer is generally written in C++ and provides functionality for the evaluation of tensor contractions, which in adcc is performed by a library of tensor operation routines (libtensor). (Epifanovsky et al., 2013) The two layers communicate by means of the pybind11 library (Jakob, Rhinelander, & Moldovan, 2017), offering a lightweight, header-only, exposure of C++ types in Python.

Implementation and efficiency of HPC-QC

VeloxChem is responsible for the construction of Fock matrices, including the underlying evaluation of two-electron integrals in AO basis, which is hybrid MPI/OpenMP parallelized

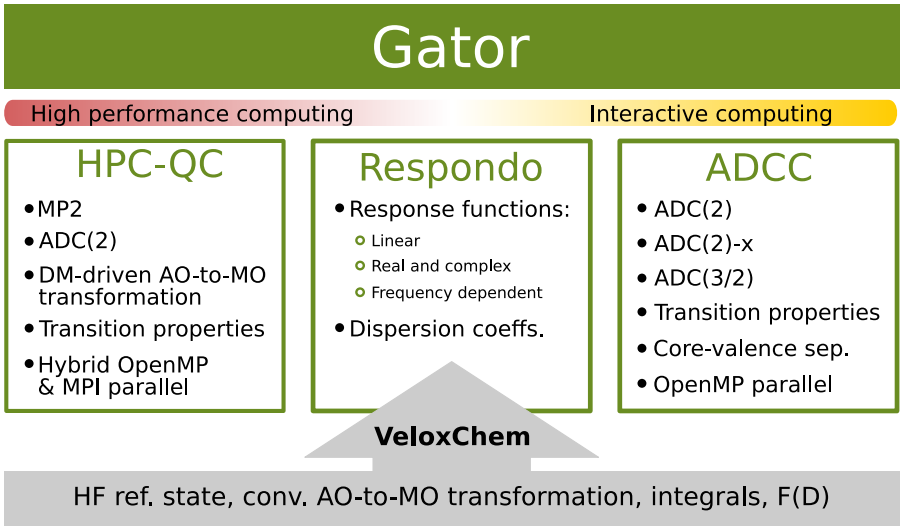

Figure 1: Gator program capabilities and module overview.

for efficient execution on HPC clusters. The module accepts, depening on memory limits, an arbitrary number of density matrices in a batch and handles those in parallel. Within a *single* evaluation of the set of two-electron integrals, the corresponding *complete batch* of Fock matrices is constructed. Such a multi-Fock-matrix construction creates additional computational cost for integral distribution. Since a larger batch size comes at the price of a reduced OpenMP parallel efficiency in the integral evaluation, it may become necessary to balance the two forms of parallelism in the integral transformation depending on the size of the system and the adopted basis set.

In the same spirit HPC-QC is *hybrid parallelized*. In regard to MO integral storage, a split MPI communicator is used across cluster nodes and any given integral naturally resides in the memory of the node executing Eq. (1), to enable usage of the aggregated memory of the available cluster nodes as well as to minimize the need for communication. For example, the storage of integral block $\langle \mathrm{oo}||\mathrm{vv}\rangle$ can be distributed over the occupied–occupied (oo) or the virtual–virtual (vv) pair-indices. The distributed storage of MO integrals allows for a parallel implementation of sigma build for ADC(2), where the tensor operations take place on the individual compute node that holds a list of distributed pair-indices and the corresponding Fock matrices in the MO basis. The construction of σ-vectors (matrix–vector product) in ADC(2) is evaluated by going through the distributed pair-indices and contracting the

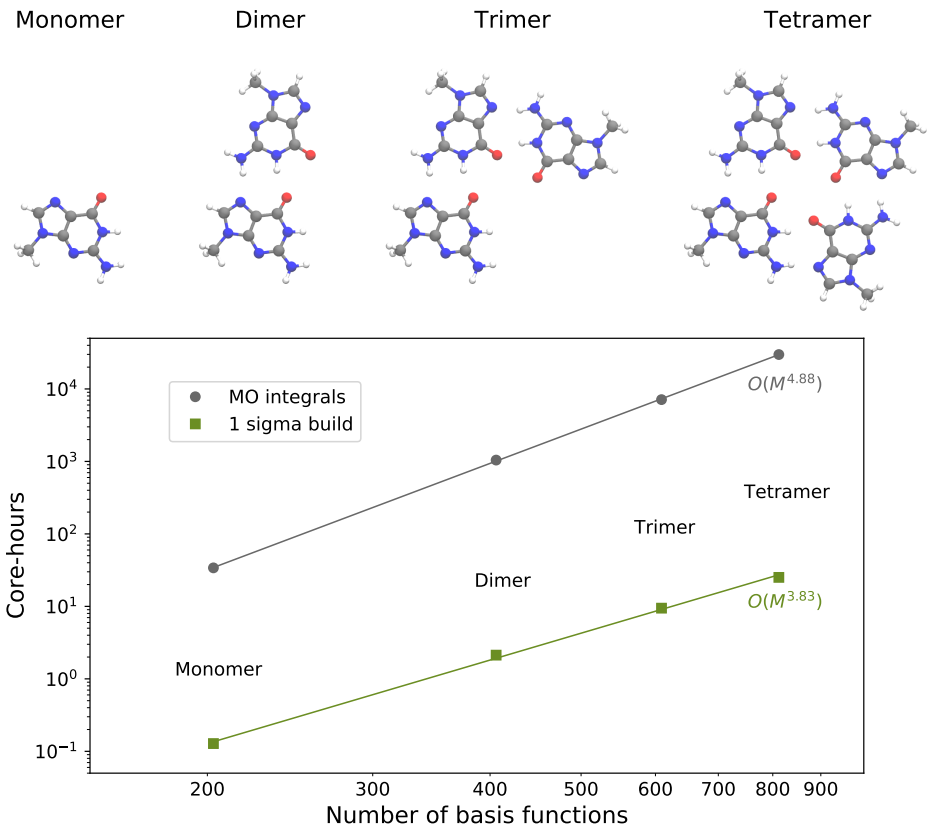

Figure 2: Scaling of the constructions of MO integrals and the ADC(2) σ-vectors with respect to the number of contracted basis functions. Results are obtained for guanine oligomers (extracted from a G-quadruplex) using the def2-SVP basis set (203 contracted basis functions per guanine). Calculations were performed on standard cluster nodes (Intel Xeon Haswell, 32 cores, 64 GB).

corresponding Fock matrices in the MO basis with the trial vectors of single excitation. The need for storing the large vector of double excitation is eliminated by packing the double excitation into the space of single excitation (Hättig & Köhn, 2002). As such, parallel ADC(2) calculation can be carried out on cluster nodes with moderate amount of memory.

In Figure 2, we show results for guanine oligomers using a basis set with highest angular momentum $l = 2$. The MO integrals calculation involves all MO integrals that are needed at the level of ADC(2) theory. We investigated the scaling of the MO integrals calculation with respect to the number of contracted basis functions (grey curve in Figure 2). For guanine

oligomers with the def2-SVP basis set, the MO integrals calculation scales as $N^{4.9}$, in line with the discussion above. The evaluation of MO integrals therefore uses the majority of the computational time (core-hours) in the parallel implementation of ADC(2), since the construction of σ-vectors show a lower scaling of $M^{3.8}$ as shown in Figure 2.

Capabilities

Calculations using the ADC(2) (Schirmer, 1982), ADC(2)-x (Trofimov & Schirmer, 1995), and ADC(3) (P. H. Harbach et al., 2014) methods can be performed using the adcc module for shared-memory architectures. MP2 energies and ADC(2) excitation energies can additionally be obtained employing the HPC-QC module using the distributed aggregated memory on HPC clusters. Electronic absorption spectra can be computed for all wavelengths ranging from the near infra-red to the soft X-ray region both by means of a "bottom-up" Davidson solver technique (Davidson, 1975) and also by addressing the absorptive part of the complex polarization propagator (CPP) (Norman, Bishop, Jensen, & Oddershede, 2001, 2005; Norman, 2011). From the real part of the CPP at imaginary frequencies, C_6 dispersion coefficients can be evaluated (Norman, Jiemchooroj, & Sernelius, 2003; Jiemchooroj, Norman, & Sernelius, 2005; Fransson, Rehn, Dreuw, & Norman, 2017). For spectrum calculations in the soft X-ray region, the core-valence-separation (CVS) is available (Cederbaum, Domcke, & Schirmer, 1980; Wenzel, Wormit, & Dreuw, 2014a, 2014b).

HOW TO USE GATOR

Gator can be used for batch-queue submission through providing a conventional input file to the Python module script as shown in Figure 3. However, we here choose to illustrate the modular, low-barrier, nature of a Python-based framework for scientific computing by, as an example, providing the calculation of the X-ray absorption spectrum of water as shown in Figure 4. This calculation was performed with the Gator program in a Jupyter notebook (Kluyver et al., 2016), which is an open, web-based interactive environment of increasing popularity. By dividing the code into multiple blocks, Jupyter enables the calculation of individual code sections, keeping results in local memory. This simplifies the rewriting and

```
@jobs
task: adc
@end

@method settings
basis: 6-311++G**
@end

@adc
tol: 1e-3
method: cvs-adc2 (cpp)
frequencies: 19.64-19.88 (0.005)
damping: 0.01
core_orbitals: 1
@end

@molecule
charge: 0
multiplicity: 1
units: angstrom
xyz:
O      0.0000000000    0.0000000000    0.1187290000
H     -0.7532010000   -0.0000000000   -0.4749160000
H      0.7532010000    0.0000000000   -0.4749160000
@end
```

Figure 3: Gator program input file for performing the same CVS-CPP-ADC(2) spectrum calculation shown in Figure 4.

recomputing of code snippets, such that the user does not need to recalculate all quantities after a modification is done. This approach allows for an interactive path to programming, analysis, and education. In Gator, we take advantage of these concepts by interactively combining *ab initio* computational spectroscopy with intuitive analysis and plotting routines through, *e.g.*, NumPy and Matplotlib (Hunter, 2007). The notebook allows for an iterative investigation of the systems at hand by varying different parameters, such as basis sets, convergence criteria, numerical solvers, and convolution/broadening functions. In addition, JupyterHub enables the spawning and management of multiple instances of single-use Jupyter notebook, as can then be done on, *e.g.*, an HPC cluster. This enables the access to data, analyses, and illustrations of results, and performing less demanding calculations on interactive cluster nodes, as well as preparing and submitting batch jobs to dedicated computational nodes. Such a hub can serve as the centralized environment for, *e.g.*, teaching a class, where the students would only need a web browser for performing computational spectroscopy studies. In addition, this framework makes the combination of several program

packages straightforward, such as molecular dynamics coupled with spectrum calculations for snapshots.

```
%matplotlib notebook
import matplotlib.pyplot as plt
import gator

gator_struct = gator.get_molecule("""
O       0.0000000000     0.0000000000     0.1187290000
H      -0.7532010000    -0.0000000000    -0.4749160000
H       0.7532010000     0.0000000000    -0.4749160000
""")
gator_basis = gator.get_molecular_basis(gator_struct,'6-311++G**')
gator_scf   = gator.run_scf(gator_struct,gator_basis,verbose=False)
gator_xas   = gator.run_adc(gator_struct,gator_basis,gator_scf,method='cvs-adc2',singlets=5,core_orbitals=1)
plt.figure(figsize=(4,5))
gator_xas.plot_spectrum()
plt.tight_layout()
```

```
                    ADC Summary of Results
                    ----------------------

+-------------------------------------------------------------+
| cvs-adc2                              singlet ,  converged  |
+-------------------------------------------------------------+
|  #       excitation energy     osc str    |v1|^2    |v2|^2  |
|          (au)           (eV)                                |
|  0      19.66388      535.0813   0.0068     0.808     0.192  |
|  1       19.7229      536.6873   0.0109    0.8021    0.1979  |
|  2      19.82636      539.5028   0.0164    0.8163    0.1837  |
|  3      19.83878      539.8407   0.0160     0.817     0.183  |
|  4      19.84596      540.0361   0.0162    0.8188    0.1812  |
+-------------------------------------------------------------+
```

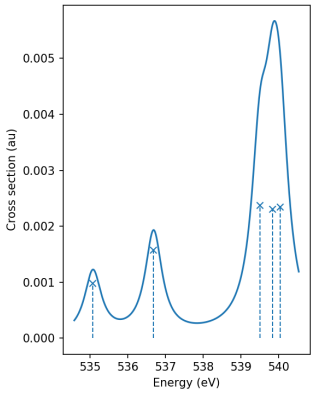

Figure 4: Gator notebook mode: The notebook input for the calculation of the X-ray absorption spectrum of water (upper left) and program output (lower left), here focusing only on information for the requested five excited states. The corresponding spectrum plot shown to the right.

NUMERICAL EXAMPLES

For linear absorption and dispersion of radiation, the molecular property of interest is the molecular polarizability. For damped response theory applied to exact states, this can be obtained from the sum-over-states expression (Norman et al., 2001, 2005; Norman, 2011)

$$\alpha_{\alpha\beta}(\omega) = \frac{1}{\hbar}\sum_{n>0}\left[\frac{\langle 0|\hat{\mu}_\alpha|n\rangle\langle n|\hat{\mu}_\beta|0\rangle}{\omega_{n0}-\omega-i\gamma_n} + \frac{\langle 0|\hat{\mu}_\beta|n\rangle\langle n|\hat{\mu}_\alpha|0\rangle}{\omega_{n0}+\omega+i\gamma_n}\right], \tag{4}$$

where $\hat{\mu}_\alpha$ is the electric-dipole operator along axis α, $\hbar\omega_{n0}$ is the transition energy between the ground state $|0\rangle$ and excited state $|n\rangle$, and γ_n corresponds to the inverse of the finite lifetime of excited state $|n\rangle$—we here assume a common parameter for all states, *i.e.*, $\gamma_n = \gamma$ yielding a Lorentzian line broadening (Norman et al., 2018). For approximate state theories such as ADC, Eq. (4) turns into different forms of matrix equations that can be found in the literature (Fransson et al., 2017). Within the electric-dipole approximation the absorption cross-section of a randomly oriented molecular system is given from the isotropic average of

the complex polarizability

$$\sigma(\omega) = \frac{\omega}{c\epsilon_0} \mathrm{Im}\left[\overline{\alpha}(\omega)\right], \tag{5}$$

thus allowing for the calculation of an absorption spectrum at arbitrary energy intervals by solving over a grid of frequencies. If instead the infinite lifetime approximation is used, *i.e.* $\gamma \to 0$, Eq. (4) becomes real, but resonance-divergent. In this case the eigenvectors and eigenvalues are determined and the spectrum is constructed with appropriate broadening schemes.

Using imaginary frequencies, the long-range dispersion interaction energy between systems A and B can be determined through the Casimir–Polder integral formula (Casimir & Polder, 1948), giving access to the C_6 dispersion coefficients

$$C_6 = \frac{3\hbar}{\pi} \int_0^\infty \overline{\alpha}_A(i\omega^I)\overline{\alpha}_B(i\omega^I) d\omega^I, \tag{6}$$

again considering randomly oriented molecular systems. This integral can be calculated using a Gauss–Legendre integration scheme with the transformation (Amos, Handy, Knowles, Rice, & Stone, 1985)

$$i\omega^I = i\omega_0(1-t)/(1+t), \tag{7}$$

with $\omega_0 = 0.3$ a.u., followed by a Gauss–Legendre quadrature in the interval $t \in [-1, 1]$. We here adopt this approach using a twelve-point integration scheme.

To illustrate the capabilities of the Gator program, we consider furan and thiophene, two isovalent aromatic molecules. We have calculated the UV/vis and X-ray absorption cross-sections, the static polarizability, and the polarizability at imaginary frequencies, as illustrated in Figure 5. A damping term $\gamma = 0.24$ eV was used for the calculation of absorption cross-sections. For comparison, the excitation energies and intensities obtained from explicit calculations of 25 eigenstates have been convoluted using a Lorentzian with the same broadening parameter. All property calculations have been done using the 6-311++G** (Krishnan, Binkley, Seeger, & Pople, 1980) basis set. The structures of the molecules have been optimized at the B3LYP (Becke, 1993)/cc-pVTZ (Dunning, 1989) level of theory using the Q-Chem 5.1 program (Shao et al., 2015).

Static polarizabilities and C_6 dispersion coefficients are important parameters, for example as input for molecular dynamics simulations. For these properties, the performance of

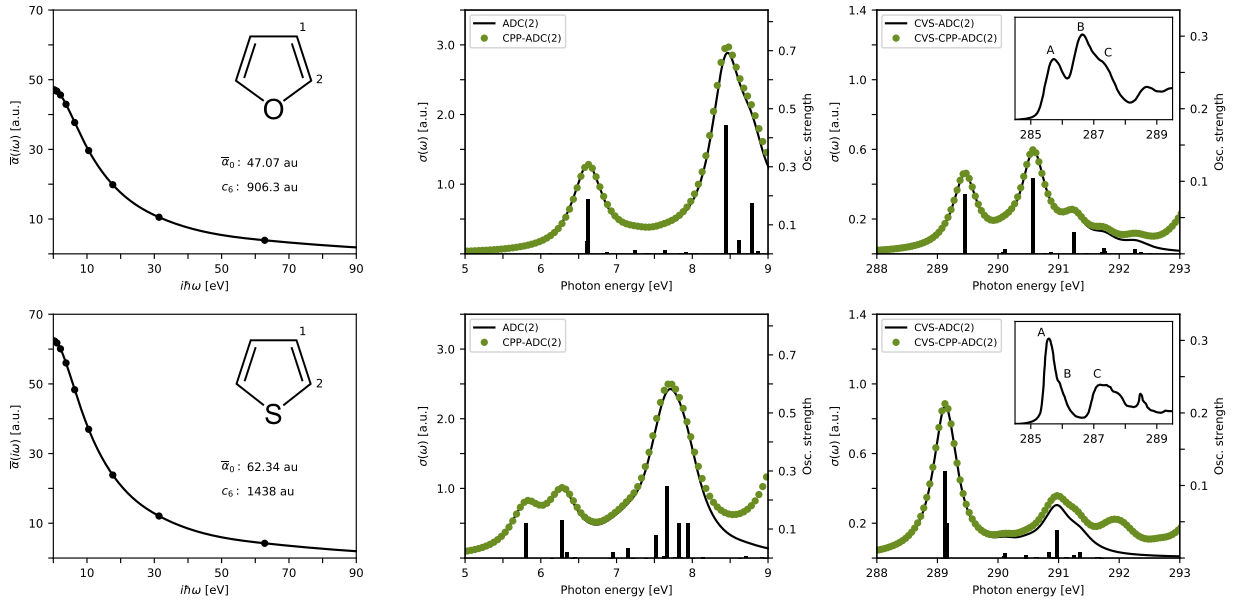

Figure 5: Properties of furan (top) and thiophene (bottom): (left) Isotropic polarizability at imaginary frequencies, $\overline{\alpha}(i\omega)$, along with the resulting C_6 dispersion coefficient from Eq. (6); (mid) UV absorption cross section, $\sigma(\omega)$, and oscillator strengths; (right) X-ray absorption cross section, $\sigma(\omega)$, and oscillator strengths at the near carbon K-edge together with insets showing the experimental spectra (Duflot et al., 2003; Grazioli et al., 2017) digitized with WebPlotDigitizer (Rohatgi, 2019).

ADC methods has already been investigated, showing good agreement with experiment (Trofimov, Krivdina, Weller, & Schirmer, 2006; Fransson et al., 2017). At complex frequencies, we obtain a smooth monotonous polarizability as illustrated in the left panels of Figure 5, featuring an isotropic static polarizability ($\overline{\alpha}_0$) and a C_6 coefficient of 47.07 and 906.3 a.u. for furan, and 62.34 and 1438 a.u. for thiophene. Experimental $\overline{\alpha}_0$:s are reported as 48.59 and 65.18 a.u. for furan and thiophene, respectively—see Ref. (Kamada et al., 2000) and references therein. That study also provides CCSD values as best theoretical estimates of 46.38 and 63.36 a.u. for furan and thiophene, respectively. Employing CCSD with a larger aug-cc-pVTZ basis set, Christiansen *et al.* reported $\overline{\alpha}_0$ for furan of 48.17 a.u. As such, the underestimation of static polarizabilities at the ADC(2)/6-311++G** level of of theory is likely to be partially explained by the choice of basis set—the study by Kamada *et al.* concluded that the electron correlation is of minor importance compared to the basis set for reproducing

experimental $\overline{\alpha}_0$:s (Kamada et al., 2000).

For the calculation of valence excitation spectra Gator offers the possibility to either solve explicitly for eigenstates or to scan over relevant frequency intervals using damped response theory. Using a Lorentzian broadening for the transitions in the first approach will result in a spectrum that is practically identical to that obtained in the second approach, as illustrated in the middle and right panels of Figure 5. The linear absorption cross-section obtained from (CVS-)CPP-ADC and the broadened eigenvalue results agree perfectly for lower energies. However, for higher energies differences between the two curves occur due to the fact that the resolved 25 eigenstates are not sufficient to obtain the full spectrum window.

The carbon K-edge spectra of furan and thiophene obtained with CVS-ADC(2) are given together with the experimental gas-phase spectra as insets of the right panels of Figure 5. Here we include the first use of CVS-CPP-ADC, which has been developed and implemented in Gator. The use of the CVS approximation on top of CPP here serves multiple purposes: (i) reduced matrix dimensions and resulting decrease in computational effort, (ii) removal of spurious valence-continuum features which may contaminate the resolved spectrum window, and (iii) circumventing difficulties in converging pure CPP-ADC calculations in the energy region of core excitations, which are strongly reduced by the introduction of the CVS scheme. The convergence issues have been observed also for CPP calculations of core excitations in the context of coupled cluster theory, and we note that the use of the CVS scheme introduces only minor scalar shift in absolute energies—for this method, element, and basis set the introduced error has been recorded as amounting to a blue-shift of ∼0.5 eV (Herbst & Fransson, 2020). As for the resulting spectra, by studying the MOs involved in the transitions or response vectors, we can assign the various features. The peak labeled A in the furan spectrum is attributed to transitions from C1, while feature B is dominated by transitions from C2. Both are assigned as $1s \rightarrow 1\pi^*$ transitions from the respective carbons, with a relative shift of 1.13 eV, in good agreement to the experimentally observed shift of 1.08 eV (Duflot et al., 2003). In terms of absolute energies, the first resonance is noted as 289.45 eV using CVS-ADC(2), as compared to experimental energy of 285.76 eV (Duflot et al., 2003). The furan spectrum is thus blue-shifted by 3.69 eV, in agreement with previous discrepancies of CVS-ADC(2) for the carbon K-edge (Wenzel et al., 2014a). Note here that relativistic effects are not included

in our calculations, which will shift transition energies upwards by approximately 0.1 eV for the carbon K-edge. Peak C of furan has been assigned to be dominated by a $2\pi^*$ transition from C1, with a shift to the C1 $1\pi^*$-resonance of 1.56 eV from experiment, or 1.72 eV from theory (Duflot et al., 2003). We obtain a shift of 1.80 eV between those two features. The spectrum of thiophene is dominated by two features, A and C, in which peak A is due to the two $1s \rightarrow 1\pi^*$ resonances. The energy shift between the two lines is 0.04 eV, in good agreement with previous TP-DFT (Grazioli et al., 2017) and MS-Xα (Hitchcock, Horsley, & Stöhr, 1986) calculations yielding 0.01 and 0.06 eV, respectively. The smaller shift between the two resonances when compared to furan is because of the less electronegative sulphur atom which changes the density around C1 and C2 to a smaller extent than the oxygen atom.

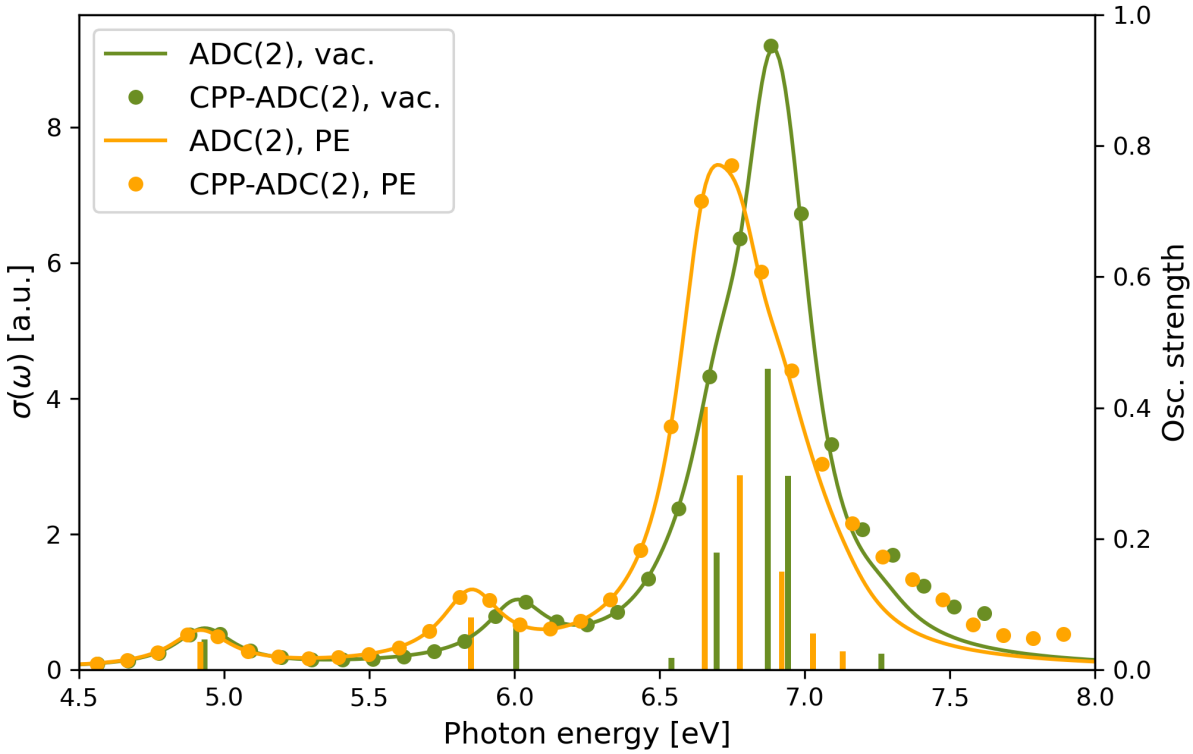

Figure 6: UV/Vis spectra of noradrenalin in vacuum and solution. Continuous lines show the convoluted stick spectra, obtained from a Lorentzian function with $\gamma = 0.124$ eV. Dots depict the one-photon absorption cross section $\sigma(\omega)$ computed with CPP.

To demonstrate the capabilities of Gator in computing absorption spectra of solvated

molecules at the ADC(2) level of theory, the spectrum of noradrenaline has been computed in gas-phase as well as in aqueous solution using the standard eigenvalue solver as well as the CPP approach. Here, the ADC(2) response equations have been solved in a similar fashion as described previously using the partial-renormalization technique to demonstrate its applicability for solving of complex response equation. The vacuum structure of noradrenalin has been optimized at the CAM-B3LYP/def2-svp (Yanai, Tew, & Handy, 2004; Weigend & Ahlrichs, 2005) level of theory as implemented in ORCA 4 (Neese, 2018), which served as input for the subsequent calculation of the seven energetically lowest singlet excited states at the ADC(2)/cc-pVDZ level of theory. Then, CPP-ADC(2) calculations were carried out on the frequency range obtained by the eigenstates with a spacing of 0.1 eV, yielding the one-photon absorption cross section for each frequency, see Figure 6.

To model the UV/Vis spectrum of noradrenaline in solution, it was placed in a box of size $48 \times 44 \times 43$ Å^3 of water molecules using packmol (Martínez, Andrade, Birgin, & Martínez, 2009) and MD simulations were carried out with NAMD 2.12 (Phillips et al., 2005) using the CHARMM 36 force field (Huang & MacKerell Jr, 2013) and parameters for noradrenalin obtained with CGenFF (Vanommeslaeghe et al., 2010). The system was equilibrated for 5 ns at 310 K and a pressure of 1 atm (NPT ensemble). A subsequent hybrid QM/MM minimization was performed with NAMD (Melo et al., 2018), where noradrenaline represented the QM region and the MM region was assigned to the solvent. The QM computations were run at the CAM-B3LYP/def2-SVP level of theory with ORCA 4 using an electrostatic embedding scheme. The final snapshot of the QM/MM minimization was extracted and parameterized using PyFramE (J. M. H. Olsen, 2018) with a standard potential model. In the spectrum calculation, the solvent effects are modeled self-consistently with the polarizable embedding (PE) model applied for the Hartree–Fock reference state (J. M. Olsen, Aidas, & Kongsted, 2010; J. M. H. Olsen & Kongsted, 2011; Scheurer et al., n.d.). The absorption spectra of noradrenaline in vacuum and solution are shown in Figure 6, where we note that energies in the latter calculation are *not* perturbatively corrected (Scheurer et al., n.d.).

GATOR FOR TRAINING AND EDUCATION

The Gator program is an ideal platform for undergraduate training and education in computational and theoretical chemistry with students ranging from the introductory bachelor to the advanced master level. It offers insight into the underlying general theory of quantum chemistry and the adopted electronic structure theory methods with a direct and concrete access of the intermediate quantities (tensor elements and wave functions) that are addressed in the workflow of quantum chemical calculations. This is accomplished by interfacing the Gator program to the student via the Jupyter notebook as described above. This allows the student to steer, control, and analyze the course of a desired quantum chemical calculation in a modular manner. Students who are initially not familiar with programming are naturally motivated to overcome barriers involved with entering the field of theory and program development. With basic knowledge of Python programming, it becomes possible via module import for students to design and implement key algorithms such as *e.g.* the SCF optimization of electron densities or the response theory calculations of excitation energies. With Gator it becomes realistic to incorporate such practical exercises into existing courses and the deepened algorithmic understanding hereby gained will be invaluable for subsequent studies at the research level.

OUTLOOK

The Gator platform will undergo development following several major lines: (i) The HPC-QC module will be extended to include implementations for the calculation of excited-state properties and the inclusion of external one-particle potentials using the intermediate state representation. (ii) The complex linear response function will be implemented in the HPC-QC module. (iii) The capabilities of the Respondo library will be further extended by including higher-order response functions to allow for simulations of advanced linear and nonlinear spectroscopies. (iv) Quantum chemical methods other than the ADC approaches will be included with a first aim at the approximate coupled cluster of second order (CC2) (Christiansen, Koch, & Jørgensen, 1995) and also equation-of-motion and linear-response

coupled cluster with singles and doubles (EOM/LR-CCSD) (Stanton & Bartlett, 1993; Koch, Kobayashi, Sanchez de Merás, & Jørgensen, 1994). (v) Modular libraries for environment models other than the PE model are under development. (vi) The engine of the HPC-QC module, *i.e.*, the efficient construction of the large number of auxiliary Fock matrices in the AO-basis, will be adapted for execution on heterogeneous cluster nodes with varying combinations of central processing units (CPUs) and graphics processing units (GPUs).

ACKNOWLEDGEMENTS

Financial support is acknowledged from the European Commission in the form of the ITN titled "*Computational Spectroscopy in Natural Sciences and Engineering (COSINE)*" (Grant No. 765739), the European Research Council (ERC) under the Horizon 2020 program (Grant No. 810367), the Swedish Research Council (Grant Nos. 2018-4343, 2017-00356, and 2017-06419), the Heidelberg Graduate School of Mathematical and Computational Methods for the Sciences (Grant No. GSC220), and the Swedish e-Science Research Centre (SeRC) as well as a fellowship from Heidelberg University for P.N. to become a visiting professor at the Interdisciplinary Center for Scientific Computing, and computational resources provided by the Swedish National Infrastructure for Computing (SNIC). Fruitful discussions with Evgeny Epifanosky and Anna I. Krylov are gratefully acknowledged.

REFERENCES

Amos, R. D., Handy, N. C., Knowles, P. J., Rice, J. E., & Stone, A. J. (1985). Ab-initio prediction of properties of CO_2, NH_3, and $CO_2 \cdots NH_3$. *J. Phys. Chem.*, *89*, 2186–2192.

Aprà, E., Bylaska, J., de Jong, W. A., Govind, N., Kowalski, K., Straatsma, T. P., ... Harrison, R. J. (2020). NWChem: Past, present, and future. *J. Chem. Phys.*, *152*, 184102.

Becke, A. D. (1993). Density-functional thermochemistry. III. The role of exact exchange. *J. Chem. Phys.*, *98*, 5648–5652.

Casimir, H. B. G., & Polder, D. (1948). The influence of retardation on the London–van der Waals forces. *Phys. Rev.*, *73*, 360–372.

Cederbaum, L. S., Domcke, W., & Schirmer, J. (1980). Many-body theory of core holes. *Phys. Rev. A*, *22*, 206–222.

Christiansen, O., Koch, H., & Jørgensen, P. (1995). The second-order approximate coupled cluster singles and doubles model CC2. *Chem. Phys. Lett.*, *243*, 409–418.

Davidson, E. R. (1975). The iterative calculation of a few of the lowest eigenvalues and corresponding eigenvectors of large real-symmetric matrices. *J. Comput. Phys.*, *17*, 87–94.

Dreuw, A. (2006). Quantum chemical methods for the investigation of photo-initiated processes in biological systems: Theory and applications. *Chem. Phys. Chem.*, *7*, 2259–2274.

Dreuw, A., & Wormit, M. (2015). The algebraic diagrammatic construction scheme for the polarization propagator for the calculation of excited states. *Wiley Interdiscip. Rev. Comput. Mol. Sci.*, *5*, 82–95.

Duflot, D., Flament, J.-P., Giuliani, A., Heinesch, J., & Hubin-Franskin, M.-J. (2003). Core shell excitation of furan at the O1s and C1s edges: An experimental and ab initio study. *J. Chem. Phys.*, *119*, 8946.

Dunning, T. H. (1989). Gaussian basis sets for use in correlated molecular calculations. I. The atoms boron through neon and hydrogen. *J. Chem. Phys.*, *90*, 1007-1023.

Epifanovsky, E., Wormit, M., Kus, T., Landau, A., Zuev, D., Khistyaev, K., ... Krylov, A. I. (2013). New implementation of high-level correlated methods using a general block-tensor library for high-performance electronic structure calculations. *J. Comp. Chem.*, *34*, 2293–2309.

Fransson, T., Rehn, D. R., Dreuw, A., & Norman, P. (2017). Static polarizabilities and C_6 dispersion coefficients using the algebraic-diagrammatic construction scheme for the complex polarization propagator. *J. Chem. Phys.*, *146*, 094301.

Gonzalez, L., Escudero, D., & Serrano-Andres, L. (2011). Progress and challenges in the calculation of electronic excited states. *Chem. Phys. Chem.*, *13*, 28–51.

Grazioli, C., Baseggio, O., Stener, M., Fronzoni, G., de Simone, M., Coreno, M., ... D'Auria,

M. (2017). Study of the electronic structure of short chain oligothiophenes. *J. Chem. Phys.*, *146*, 054303.

Grunenberg, J. (2010). *Computational spectroscopy: methods, experiments and applications.* Wiley VCH.

Harbach, P. H., Wormit, M., & Dreuw, A. (2014). The third-order algebraic diagrammatic construction method (ADC(3)) for the polarization propagator for closed-shell molecules: Efficient implementation and benchmarking. *J. Chem. Phys.*, *141*(6), 064113.

Harbach, P. H. P., & Dreuw, A. (2011). The art of choosing the right quantum chemical excited-state method for large molecular systems. In P. Comba (Ed.), *Modelling of Molecular Properties* (pp. 29–47). Wiley VCH.

Hättig, C., & Köhn, A. (2002). Transition moments and excited-state first-order properties in the coupled-cluster model cc2 using the resolution-of-the-identity approximation. *J. Chem. Phys.*, *117*, 6939–6951. doi: 10.1063/1.1506918

Herbst, M. F. (2018). *Development of a modular quantum-chemistry framework for the investigation of novel basis functions* (Doctoral dissertation, Ruprecht-Karls-Universität Heidelberg). doi: 10.11588/heidok.00024519

Herbst, M. F., Dreuw, A., & Avery, J. E. (2018). Towards quantum-chemical method development for arbitrary basis functions. *J. Chem. Phys.*, *149*(8), 84106. doi: 10.1063/1.5044765

Herbst, M. F., & Fransson, T. (2020). Quantifying the error of the core-valence separation approximation. *J. Chem. Phys.*.

Herbst, M. F., Scheurer, M., Fransson, T., Rehn, D. R., & Dreuw, A. (2020). adcc: A versatile toolkit for rapid development of algebraic-diagrammatic construction methods. *Wiley Interdiscip. Rev. Comput. Mol. Sci.*, e1462. doi: 10.1002/wcms.1462

Hitchcock, A. P., Horsley, J. A., & Stöhr, J. (1986). Inner shell excitation of thiophene and thiolane: Gas, solid, and monolayer states. *J. Chem. Phys.*, *85*, 4835–4848.

Holthausen, M., & Koch, W. (2001). *A Chemist's guide to density functional theory.* Wiley VCH.

Huang, J., & MacKerell Jr, A. D. (2013). Charmm36 all-atom additive protein force field:

Validation based on comparison to nmr data. *Journal of computational chemistry*, *34*(25), 2135–2145.

Hunter, J. D. (2007). Matplotlib: A 2D graphics environment. *Computing In Science & Engineering*, *9*(3), 90–95.

Jakob, W., Rhinelander, J., & Moldovan, D. (2017). *pybind11 – Seamless operability between C++11 and Python.* Retrieved from https://github.com/pybind/pybind11

Jiemchooroj, A., Norman, P., & Sernelius, B. E. (2005). Complex polarization propagator method for calculation of dispersion coefficients of extended π-conjugated systems: The C[sub 6] coefficients of polyacenes and C[sub 60]. *J. Chem. Phys.*, *123*(12), 124312. Retrieved from http://link.aip.org/link/JCPSA6/v123/i12/p124312/s1&Agg=doi doi: 10.1063/1.2035589

Jones, E., Oliphant, T., & Peterson, P. (2001). *SciPy: Open source scientific tools for Python.* Retrieved from http://www.scipy.org/

Kamada, K., Ueda, M., Nagao, H., Tawa, K., Sugino, T., Schmizu, Y., & Ohta, K. (2000). Molecular design for organic nonlinear optics: Polarizability and hyperpolarizabilities of furan homologues investigated by ab initio molecular orbital method. *J. Phys. Chem. A*, *104*, 4723–4734.

Kluyver, T., Ragan-Kelley, B., Pérez, F., Granger, B., Bussonnier, M., Frederic, J., ... Jupyter Development Team (2016). *Jupyter Notebooks—a publishing format for reproducible computational workflows.* Retrieved from https://jupyter.org/

Koch, H., Kobayashi, R., Sanchez de Merás, A., & Jørgensen, P. (1994). Calculation of size-intensive transition moments from the coupled cluster singles and doubles linear response function. *J. Chem. Phys.*, *100*, 4393–4400.

Krishnan, R., Binkley, J. S., Seeger, R., & Pople, J. A. (1980). Self-consistent molecular orbital methods. XX. A basis set for correlated wave functions. *J. Chem. Phys.*, *72*, 650–654.

Lewis, C. A., Calvin, J. A., & Valeev, E. F. (2016). Clustered low-rank tensor format: Introduction and application to fast construction of Hartree–Fock exchange. *J. Chem. Theory Comput.*, *12*, 5868–5880.

Mardirossiana, N., & Head-Gordon, M. (2017). Thirty years of density functional the-

ory in computational chemistry: an overview and extensive assessment of 300 density functionals. *Mol. Phys.*, *115*, 2315-2372.

Martínez, L., Andrade, R., Birgin, E. G., & Martínez, J. M. (2009). Packmol: a package for building initial configurations for molecular dynamics simulations. *Journal of computational chemistry*, *30*(13), 2157–2164.

Melo, M. C., Bernardi, R. C., Rudack, T., Scheurer, M., Riplinger, C., Phillips, J. C., ... Luthey-Schulten, Z. (2018). NAMD goes quantum: An integrative suite for hybrid simulations. *Nat. Methods*, *15*(5), 351–354. doi: 10.1038/nmeth.4638

Neese, F. (2018). Software update: the orca program system, version 4.0. *Wiley Interdisciplinary Reviews: Computational Molecular Science*, *8*(1), e1327.

Norman, P. (2011). A perspective on nonresonant and resonant electronic response theory for time-dependent molecular properties. *Phys. Chem. Chem. Phys.*, *13*, 20519–20535.

Norman, P., Bishop, D. M., Jensen, H. J. A., & Oddershede, J. (2001). Near-resonant absorption in the time-dependent self-consistent field and multiconfigurational self-consistent field approximations. *J. Chem. Phys.*, *115*, 10323–10334.

Norman, P., Bishop, D. M., Jensen, H. J. A., & Oddershede, J. (2005). Nonlinear response theory with relaxation: the first-order hyperpolarizability. *J. Chem. Phys.*, *123*, 194103.

Norman, P., Jiemchooroj, A., & Sernelius, B. E. (2003). Polarization propagator calculations of the polarizability tensor at imaginary frequencies and long-range interactions for the noble gases and n-alkanes. *J. Chem. Phys.*, *118*(20), 9167. Retrieved from http://link.aip.org/link/JCPSA6/v118/i20/p9167/s1&Agg=doi doi: 10.1063/1.1568082

Norman, P., Ruud, K., & Saue, T. (2018). *Principles and practices of molecular properties*. Chichester, UK: John Wiley & Sons, Ltd.

Olsen, J. M., Aidas, K., & Kongsted, J. (2010). Excited States in Solution through Polarizable Embedding. *J. Chem. Theory Comput.*, *6*(12), 3721–3734.

Olsen, J. M. H. (2018). *PyFraME: Python tools for Fragment-based Multiscale Embedding (version 0.1.0)*. doi: https://doi.org/10.5281/zenodo.293765

Olsen, J. M. H., & Kongsted, J. (2011). *Molecular Properties through Polarizable Embedding* (Vol. 61). doi: 10.1016/B978-0-12-386013-2.00003-6

Olsen, J. M. H., Reine, S., Vahtras, O., Kjellgren, E., Reinholdt, P., Hjorth Dundas, K. O., ... Norman, P. (2020, jun). Dalton Project: A Python platform for molecular- and electronic-structure simulations of complex systems. *J. Chem. Phys.*, *152*(21), 214115. Retrieved from https://doi.org/10.1063/1.5144298{%}0Ahttp://aip.scitation.org/doi/10.1063/1.5144298http://aip.scitation.org/doi/10.1063/1.5144298 doi: 10.1063/1.5144298

Peng, C., Calvin, J. A., Pavosevic, F., Zhang, J., & Valeev, E. F. (2016). Massively parallel implementation of explicitly correlated coupled-cluster singles and doubles using tiledarray framework. *J. Phys. Chem. A*, *120*, 10231–10244.

Peng, C., Lewis, C. A., Wang, X., Clement, M. C., Pierce, K., Rishi, V., ... Valeev, E. F. (2020). Massively parallel quantum chemistry: A high-performance research platform for electronic structure. *J. Chem. Phys.*, *153*, 044120.

Phillips, J. C., Braun, R., Wang, W., Gumbart, J., Tajkhorshid, E., Villa, E., ... Schulten, K. (2005). Scalable molecular dynamics with namd. *Journal of computational chemistry*, *26*(16), 1781–1802.

Rinkevicius, Z., Li, X., Vahtras, O., Ahmadzadeh, K., Brand, M., Ringholm, M., ... Norman, P. (2020). Veloxchem: A python-driven density-functional theory program for spectroscopy simulations in high-performance computing environments. *Wiley Interdiscip. Rev. Comput. Mol. Sci.*, *10*(5), e1457. doi: 10.1002/wcms.1457

Rohatgi, A. (2019). *WebPlotDigitizer.* Retrieved from https://automeris.io/WebPlotDigitizer

Scheurer, M., Herbst, M., Reinholdt, P., Olsen, J. M., Dreuw, A., & Kongsted, J. (n.d.). Polarizable Embedding Combined with the Algebraic Diagrammatic Construction: Tackling Excited States in Biomolecular Systems. *J. Chem. Theory Comput.*, *14*(9), 4870 – 4883. doi: 10.1021/acs.jctc.8b00576

Schirmer, J. (1982). Beyond the random-phase approximation: a new approximation scheme for the polarization propagator. *Phys. Rev. A*, *26*, 2395–2416.

Shao, Y., Gan, Z., Epifanovsky, E., Gilbert, A. T. B., Wormit, M., Kussmann, J., ... Head-Gordon, M. (2015). Advance in molecular quantum chemistry contained in the Q-Chem 4 program package. *Mol. Phys.*, *113*, 184–215.

Smith, D. G. A., Burns, L. A., Simmonett, A. C., Parrish, R. M., Schieber, M. C., Galvelis, R., ... Sherrill, C. D. (2020). PSI4 1.4: Open-source software for high-throughput quantum chemistry. *J. Chem. Phys.*, *152*, 184108.

Smith, D. G. A., Burns, L. A., Sirianni, D. A., Nascimento, D. R., Kumar, A., James, A. M., ... Sherrill, C. D. (2018). Psi4NumPy: An interactive quantum chemistry programming environment for reference implementations and rapid development. *J. Chem. Theory Comput.*, *14*(7), 3504–3511.

Stanton, J. F., & Bartlett, R. J. (1993). Equation of motion coupled-cluster method: A systematic biorthogonal approach to molecular excitation energies, transition probabilities, and excited state properties. *J. Chem. Phys.*, *98*, 7029–7039.

Sun, Q., Berkelbach, T. C., Blunt, N. S., Booth, G. H., Guo, S., Li, Z., ... Chan, G. K.-L. (2018). PySCF: the Python-based simulations of chemistry framework. *Wiley Interdiscip. Rev. Comput. Mol. Sci.*, *8*(1), e1340.

Sun, Q., Zhang, X., Banerjee, S., Bao, P., Barbry, M., Blunt, N. S., ... Chan, G. K.-L. (2020). Recent developments in the PySCF program package. *J. Chem. Phys.*, *153*, 024109.

Trofimov, A. B., Krivdina, I. L., Weller, J., & Schirmer, J. (2006). Algebraic-diagrammatic construction propagator approach to molecular response properties. *Chem. Phys.*, *329*, 1–10.

Trofimov, A. B., & Schirmer, J. (1995). An efficient polarization propagator approach to valence electron excitation spectra. *J. Phys. B At. Mol. Opt. Phys.*, *28*, 2299–2324.

van der Walt, S., Chris Colbert, S., & Varoquaux, G. (2011). The NumPy array: A structure for efficient numerical computation. *Comput. Sci. Eng.*, *13*(2), 22–30.

Vanommeslaeghe, K., Hatcher, E., Acharya, C., Kundu, S., Zhong, S., Shim, J., ... Mackerell Jr., A. D. (2010). Charmm general force field: A force field for drug-like molecules compatible with the charmm all-atom additive biological force fields. *Journal of Computational Chemistry*, *31*(4), 671-690. Retrieved from https://onlinelibrary.wiley.com/doi/abs/10.1002/jcc.21367 doi: 10.1002/jcc.21367

Weigend, F., & Ahlrichs, R. (2005). Balanced basis sets of split valence, triple zeta valence and quadruple zeta valence quality for H to Rn: Design and assessment of accuracy.

Phys. Chem. Chem. Phys.. doi: 10.1039/b508541a

Wenzel, J., Wormit, M., & Dreuw, A. (2014a). Calculating core-level excitations and X-ray absorption spectra of medium-sized closed-shell molecules with the algebraic-diagrammatic construction scheme for the polarization propagator. *J. Comput. Chem.*, *35*, 1900–1915.

Wenzel, J., Wormit, M., & Dreuw, A. (2014b). Calculating X-ray absorption spectra of open-shell molecules with the unrestricted algebraic-diagrammatic construction scheme for the polarization propagator. *J. Chem. Theory Comput.*, *10*, 4583–4598.

Yanai, T., Tew, D. P., & Handy, N. C. (2004, jul). A new hybrid exchange–correlation functional using the Coulomb-attenuating method (CAM-B3LYP). *Chem. Phys. Lett.*, *393*(1-3), 51–57. Retrieved from http://linkinghub.elsevier.com/retrieve/pii/S0009261404008620 doi: 10.1016/j.cplett.2004.06.011